Research Article | Vol. 26, No. 18 | 3 Sep 2018 | OPTICS EXPRESS 23333

Optics EXPRESS

Self-error-corrected hyperparallel photonic quantum computation working with both the polarization and the spatial-mode degrees of freedom

GUAN-YU WANG,[1] TAO LI,[2] QING AI,[1] AND FU-GUO DENG[1,*]

[1]*Department of Physics, Applied Optics Beijing Area Major Laboratory, Beijing Normal University, Beijing 100875, China*

[2]*School of Science, Nanjing University of Science and Technology, Nanjing 210094, China*

[*]*fgdeng@bnu.edu.cn*

Abstract: Usually, the hyperparallel quantum computation can speed up quantum computing, reduce the quantum resource consumed largely, resist to noise, and simplify the storage of quantum information. Here, we present the first scheme for the self-error-corrected hyperparallel photonic quantum computation working with both the polarization and the spatial-mode degrees of freedom of photon systems simultaneously. It can prevent bit-flip errors from happening with an imperfect nonlinear interaction in the nearly realistic condition. We give the way to design the universal hyperparallel photonic quantum controlled-NOT (CNOT) gate on a two-photon system, resorting to the nonlinear interaction between the circularly polarized photon and the electron spin in the quantum dot in a double-sided microcavity system, by taking the imperfect interaction in the nearly realistic condition into account. Its self-error-corrected pattern prevents the bit-flip errors from happening in the hyperparallel quantum CNOT gate, guarantees the robust fidelity, and relaxes the requirement for its experiment. Meanwhile, this scheme works in a failure-heralded way. Also, we generalize this approach to achieve the self-error-corrected hyperparallel quantum CNOT^N gate working on a multiple-photon system. These good features make this scheme more useful in the photonic quantum computation and quantum communication in the future.

OCIS codes: (270.0270) Quantum optics; (270.5585) Quantum information and processing; (270.5565) Quantum communications.

References and links

1. P. W. Shor, "Algorithms for quantum computation: discrete logarithms and factoring," in *Proceedings of the 35th Annual Symposium on Foundations of Computer Science*, S. Goldwasser, ed. (IEEE Computer Society Press, 1994), pp. 124–134.
2. L. K. Grover, "Quantum mechanics helps in searching for a needle in a haystack," Phys. Rev. Lett. **79**, 325–328 (1997).
3. G. L. Long, "Grover algorithm with zero theoretical failure rate," Phys. Rev. A **64**, 022307 (2001).
4. E. Knill, R. Laflamme, and G. J. Milburn, "A scheme for efficient quantum computation with linear optics," Nature **409**, 46–52 (2001).
5. M. A. Nielsen, "Optical quantum computation using cluster states," Phys. Rev. Lett. **93**, 040503 (2004).
6. Y. X. Gong, G. C. Guo, and T. C. Ralph, "Methods for a linear optical quantum Fredkin gate," Phys. Rev. A **78**, 012305 (2008).
7. J. L. O' Brien, G. J. Pryde, A. G. White, T. C. Ralph, and D. Branning, "Demonstration of an all-optical quantum controlled-NOT gate," Nature **426**, 264–267 (2003).
8. S. Gasparoni, J. W. Pan, P. Walther, T. Rudolph, and A. Zeilinger, "Realization of a photonic controlled-NOT gate sufficient for quantum computation," Phys. Rev. Lett. **93**, 020504 (2004).
9. K. Nemoto and W. J. Munro, "Nearly deterministic linear optical controlled-NOT gate," Phys. Rev. Lett. **93**, 250502 (2004).
10. X. Q. Li, Y. W. Wu, D. Steel, D. Gammon, T. H. Stievater, D. S. Katzer, D. Park, C. Piermarocchi, and L. J. Sham, "An all-optical quantum gate in a semiconductor quantum dot," Science **301**, 809–811 (2003).

#330720 https://doi.org/10.1364/OE.26.023333
Journal © 2018 Received 1 May 2018; revised 28 Jun 2018; accepted 20 Jul 2018; published 27 Aug 2018

Optics EXPRESS

11. H. R. Wei and F. G. Deng, "Scalable photonic quantum computing assisted by quantum-dot spin in double-sided optical microcavity," Opt. Express **21**, 17671–17685 (2013).
12. C. Wang, Y. Zhang, R. Z. Jiao, and G. S. Jin, "Universal quantum controlled phase gate on photonic qubits based on nitrogen vacancy centers and microcavity resonators," Opt. Express **21**, 19252–19260 (2013).
13. Y. H. Kang, Y. Xia, and P. M. Lu, "Two-photon phase gate with linear optical elements and atom-cavity system," Quantum Inf. Process. **15**, 4521–4535 (2016).
14. D. Jaksch, H. J. Briegel, J. I. Cirac, C. W. Gardiner, and P. Zoller, "Entanglement of atoms via cold controlled collisions," Phys. Rev. Lett. **82**, 1975–1978 (1999).
15. D. Jaksch, J. I. Cirac, P. Zoller, S. L. Rolston, R. Côté, and M. D. Lukin, "Fast quantum gates for neutral atoms," Phys. Rev. Lett. **85**, 2208–2211 (2000).
16. L. Isenhower, E. Urban, X. L. Zhang, A. T. Gill, T. Henage, T. A. Johnson, T. G. Walker, and M. Saffman, "Demonstration of a neutral atom controlled-NOT quantum gate," Phys. Rev. Lett. **104**, 010503 (2010).
17. A. S. Sørensen and K. Mølmer, "Measurement induced entanglement and quantum computation with atoms in optical cavities," Phys. Rev. Lett. **91**, 097905 (2003).
18. H. F. Wang, A. D. Zhu, and S. Zhang, "One-step implementation of a multiqubit phase gate with one control qubit and multiple target qubits in coupled cavities," Opt. Lett. **39**, 1489–1492 (2014).
19. Y. Li, L. Aolita, D. E. Chang, and L. C. Kwek, "Robust-fidelity atom-photon entangling gates in the weak-coupling regime," Phys. Rev. Lett. **109**, 160504 (2012).
20. J. Borregaard, P. Kómár, E. M. Kessler, A. S. Sørensen, and M. D. Lukin, "Heralded quantum gates with integrated error detection in optical cavities," Phys. Rev. Lett. **114**, 110502 (2015).
21. W. Qin, X. Wang, A. Miranowicz, Z. Zhong, and F. Nori, "Heralded quantum controlled-phase gates with dissipative dynamics in macroscopically distant resonators," Phys. Rev. A **96**, 012315 (2017).
22. J. Song, Y. Xia, and H. S. Song, "Quantum gate operations using atomic qubits through cavity input-output process," Europhys. Lett. **87**, 50005 (2009).
23. D. Loss and D. P. DiVincenzo, "Quantum computation with quantum dots," Phys. Rev. A **57**, 120–126 (1998).
24. A. Imamoglu, D. D. Awschalom, G. Burkard, D. P. DiVincenzo, D. Loss, M. Sherwin, and A. Small, "Quantum information processing using quantum dot spins and cavity QED," Phys. Rev. Lett. **83**, 4204–4207 (1999).
25. C. Y. Hu, W. J. Munro, and J. G. Rarity, "Deterministic photon entangler using a charged quantum dot inside a microcavity," Phys. Rev. B **78**, 125318 (2008).
26. C. Y. Hu, W. J. Munro, J. L. O'Brien, and J. G. Rarity, "Proposed entanglement beam splitter using a quantum-dot spin in a double-sided optical microcavity," Phys. Rev. B **80**, 205326 (2009).
27. H. R. Wei and F. G, Deng, "Universal quantum gates on electron-spin qubits with quantum dots inside single-side optical microcavities," Opt. Express **22**, 593–607 (2014).
28. T. Li and F. G. Deng, "Error-rejecting quantum computing with solid-state spins assisted by low-Q optical microcavities," Phys. Rev. A **94**, 062310 (2016).
29. T. van der Sar, Z. H. Wang, M. S. Blok, H. Bernien, T. H. Taminiau, D. M. Toyli, D. A. Lidar, D. D. Awschalom, R. Hanson, and V. V. Dobrovitski, "Decoherence-protected quantum gates for a hybrid solid-state spin register," Nature **484**, 82–86 (2012).
30. H. R. Wei and F. G. Deng, "Compact quantum gates on electron-spin qubits assisted by diamond nitrogen-vacancy centers inside cavities," Phys. Rev. A **88**, 042323 (2013).
31. N. A. Gershenfeld and I. L. Chuang, "Bulk spin-resonance quantum computation," Science **275**, 350–356 (1997).
32. D. G. Cory, A. F. Fahmy, and T. F. Havel, "Ensemble quantum computing by NMR-spectroscopy," Proc. Natl. Acad. Sci. United States Am. **94**, 1634–1639 (1997).
33. I. L. Chuang, N. Gershenfeld, M. G. Kubinec, and D. W. Leung, "Bulk quantum computation with nuclear magnetic resonance: theory and experiment," Proceeding Royal Soc. A **454**, 447–467 (1998).
34. R. Schack and C. M. Caves, "Classical model for bulk-ensemble NMR quantum computation," Phys. Rev. A **60**, 4354–4362 (1999).
35. J. A. Jones, V. Vedral, A. Ekert, and G. Castagnoli, "Geometric quantum computation using nuclear magnetic resonance," Nature **403**, 869–871 (2000).
36. G. R. Feng, G. F. Xu, and G. L. Long, "Experimental realization of nonadiabatic holonomic quantum computation," Phys. Rev. Lett. **110**, 190501 (2013).
37. Y. Long, G. R. Feng, Y. C. Tang, W. Qin, and G. L. Long, "NMR realization of adiabatic quantum algorithms for the modified simon problem," Phys. Rev. A **88**, 012306 (2013).
38. L. Marrucci, C. Manzo, and D. Paparo, "Optical spin-to-orbital angular momentum conversion in inhomogeneous anisotropic media," Phys. Rev. Lett. **96**, 163905 (2006).
39. E. Nagali, F. Sciarrino, F. De Martini, L. Marrucci, B. Piccirillo, E. Karimi, and E. Santamato, "Quantum information transfer from spin to orbital angular momentum of photons," Phys. Rev. Lett. **103**, 013601 (2009).
40. A. R. C. Pinheiro, C. E. R. Souza, D. P. Caetano, J. A. O. Huguenin, A. G. M. Schmidt, and A. Z. Khoury, "Vector vortex implementation of a quantum game," J. Opt. Soc. Am. B **30**, 3210–3214 (2013).
41. G. Milione, T. A. Nguyen, J. Leach, D. A. Nolan, and R. Alfano, "Using the nonseparability of vector beams to encode information for optical communication," Opt. Lett. **40**, 4887–4890 (2015).
42. W. F. Balthazar, C. E. R. Souza, D. P. Caetano, E. F. Galvão, J. A. O. Huguenin, and A. Z. Khoury, "Tripartite nonseparability in classical optics," Opt. Lett. **41**, 5797–5800 (2016).

Optics EXPRESS

43. G. Vallone, R. Ceccarelli, F. De Martini, and P. Mataloni, "Hyperentanglement of two photons in three degrees of freedom," Phys. Rev. A **79**, 030301 (2009).
44. D. Bhatti, J. von Zanthier, and G. S. Agarwal, "Entanglement of polarization and orbital angular momentum," Phys. Rev. A **91**, 062303 (2015).
45. J. T. Barreiro, N. K. Langford, N. A. Peters, and P. G. Kwiat, "Generation of hyperentangled photon pairs," Phys. Rev. Lett. **95**, 260501 (2005).
46. C. Cinelli, M. Barbieri, F. De Martini, and P. Mataloni, "Realization of hyperentangled two-photon states," Laser Phys. **15**, 124–128 (2005).
47. M. Barbieri, C. Cinelli, F. De Martini, and P. Mataloni, "Generation of (2×2) and (4×4) two-photon states with tunable degree of entanglement and mixedness," Fortschritte der Physik **52**, 1102ÂÍC1109 (2004).
48. M. Barbieri, C. Cinelli, P. Mataloni, and F. De Martini, "Polarization-momentum hyperentangled states: Realization and characterization," Phys. Rev. A **72**, 052110 (2005).
49. A. Rossi, G. Vallone, A. Chiuri, F. De Martini, and P. Mataloni, "Multipath entanglement of two photons," Phys. Rev. Lett. **102**, 153902 (2009).
50. F. G. Deng, B. C. Ren, and X. H. Li, "Quantum hyperentanglement and its applications in quantum information processing," Sci. Bull. **62**, 46–68 (2017).
51. Y. Q. He, D. Ding, P. Tao, F. L. Yan, and T. Gao, "Generation of four-photon hyperentangled state using spontaneous parametric down-conversion source with the second-order term," Acta Phys. Sin. **67**, 060302 (2018).
52. B. Coutinho dos Santos, K. Dechoum, and A. Z. Khoury, "Continuous-variable hyperentanglement in a parametric oscillator with orbital angular momentum," Phys. Rev. Lett. **103**, 230503 (2009).
53. K. Liu, J. Guo, C. X. Cai, S. F. Guo, and J. R. Gao, "Experimental Generation of Continuous-Variable Hyperentanglement in an Optical Parametric Oscillator," Phys. Rev. Lett. **113**, 170501 (2014).
54. B. C. Ren, H. R. Wei, and F. G. Deng, "Deterministic photonic spatial-polarization hyper-controlled-not gate assisted by a quantum dot inside a one-side optical microcavity," Laser Phys. Lett. **10**, 095202 (2013).
55. B. C. Ren and F. G. Deng, "Hyper-parallel photonic quantum computation with coupled quantum dots," Sci. Rep. **4**, 4623 (2014).
56. T. J. Wang, Y. Zhang, and C. Wang, "Universal hybrid hyper-controlled quantum gates assisted by quantum dots in optical double-sided microcavities," Laser Phys. Lett. **11**, 025203 (2014).
57. B. C. Ren, G. Y. Wang, and F. G. Deng, "Universal hyperparallel hybrid photonic quantum gates with dipole-induced transparency in the weak-coupling regime," Phys. Rev. A **91**, 032328 (2015).
58. T. Li and G. L. Long, "Hyperparallel optical quantum computation assisted by atomic ensembles embedded in double-sided optical cavities," Phys. Rev. A **94**, 022343 (2016).
59. C. Y. Hu, A. Young, J. L. O'Brien, W. J. Munro, and J. G. Rarity, "Giant optical Faraday rotation induced by a single-electron spin in a quantum dot: applications to entangling remote spins via a single photon," Phys. Rev. B **78**, 085307 (2008).
60. J. R. Petta, A. C. Johnson, J. M. Taylor, E. A. Laird, A. Yacoby, M. D. Lukin, C. M. Marcus, M. P. Hanson, and A. C. Gossard, "Coherent manipulation of coupled electron spins in semiconductor quantum dots," Science **309**, 2180–2184 (2005).
61. A. Greilich, D. R. Yakovlev, A. Shabaev, A. L. Efros, I. A. Yugova, R. Oulton, V. Stavarache, D. Reuter, A. Wieck, and M. Bayer, "Mode locking of electron spin coherences in singly charged quantum dots," Science **313**, 341–345 (2006).
62. J. M. Elzerman, R. Hanson, L. H. Willems van Beveren, B. Witkamp, L. M. K. Vandersypen, and L. P. Kouwenhoven, "Single-shot read-out of an individual electron spin in a quantum dot," Nature **430**, 431–435 (2004).
63. M. Kroutvar, Y. Ducommun, D. Heiss, M. Bichler, D. Schuh, G. Abstreiter, and J. J. Finley, "Optically programmable electron spin memory using semiconductor quantum dots," Nature **432**, 81–84 (2004).
64. M. Atatüre, J. Dreiser, A. Badolato, A. Högele, K. Karrai, and A. Imamoglu, "Quantum-dot spin-state preparation with near-unity fidelity," Science **312**, 551–553 (2006).
65. M. Atatüre, J. Dreiser, A. Badolato, and A. Imamoglu, "Observation of faraday rotation from a single confined spin," Nat. Phys. **3**, 101–106 (2007).
66. J. Berezovsky, M. H. Mikkelsen, N. G. Stoltz, L. A. Coldren, and D. D. Awschalom, "Picosecond coherent optical manipulation of a single electron spin in a quantum dot," Science **320**, 349–352 (2008).
67. D. Press, T. D. Ladd, B. Y. Zhang, and Y. Yamamoto, "Complete quantum control of a single quantum dot spin using ultrafast optical pulses," Nature **456**, 218–221 (2008).
68. J. A. Gupta, R. Knobel, N. Samarth, and D. D. Awschalom, "Ultrafast manipulation of electron spin coherence," Science **292**, 2458–2461 (2001).
69. P. C. Chen, C. Piermarocchi, L. J. Sham, D. Gammon, and D. G. Steel, "Theory of quantum optical control of a single spin in a quantum dot," Phys. Rev. B **69**, 075320 (2004).
70. R. Hanson, L. H. Willems van Beveren, I. T. Vink, J. M. Elzerman, W. J. M. Naber, F. H. L. Koppens, L. P. Kouwenhoven, and L. M. K. Vandersypen, "Single-shot readout of electron spin states in a quantum dot using spin-dependent tunnel rates," Phys. Rev. Lett. **94**, 196802 (2005).
71. D. F. Walls and G. J. Milburn, *Quantum Optics* (Springer-Verlag, 1994).
72. J. H. An, M. Feng, and C. H. Oh, "Quantum-information processing with a single photon by an input-output process with respect to low-Q cavities," Phys. Rev. A **79**, 032303 (2009).

Optics EXPRESS

73. C. Y. Hu and J. G. Rarity, "Loss-resistant state teleportation and entanglement swapping using a quantum-dot spin in an optical microcavity," Phys. Rev. B **83**, 115303 (2011).
74. D. Press, K. De Greve, P. L. McMahon, T. D. Ladd, B. Friess, C. Schneider, M. Kamp, S. Höfling, A. Forchel, and Y. Yamamoto, "Ultrafast optical spin echo in a single quantum dot," Nat. Photonics **4**, 367–370 (2010).
75. G. Bester, S. Nair, and A. Zunger, "Pseudopotential calculation of the excitonic fine structure of million-atom self-assembled $In_{1-x}Ga_xAs/GaAs$ quantum dots," Phys. Rev. B **67**, 161306 (2003).
76. I. J. Luxmoore, E. D. Ahmadi, B. J. Luxmoore, N. A.Wasley, A. I. Tartakovskii, M. Hugues, M. S. Skolnick, and A. M. Fox, "Restoring mode degeneracy in H1 photonic crystal cavities by uniaxial strain tuning," Appl. Phys. Lett. **100**, 121116 (2012).
77. C. Bonato, E. van Nieuwenburg, J. Gudat, S. Thon, H. Kim, M. P. van Exter, and D. Bouwmeester, "Strain tuning of quantum dot optical transitions via laser-induced surface defects," Phys. Rev. B **84**, 075306 (2011).
78. K. Hennessy, C. Högerle, E. Hu, A. Badolato, and A. Imamoğlu, "Tuning photonic nanocavities by atomic force microscope nano-oxidation," Appl. Phys. Lett. **89**, 041118 (2006).
79. Y. Eto, A. Noguchi, P. Zhang, M. Ueda, and M. Kozuma, "Projective measurement of a single nuclear spin qubit by using two-mode cavity QED," Phys. Rev. Lett. **106**, 160501 (2011).
80. M. Hall, J. Altepeter, and P. Kumar, "Ultrafast switching of photonic entanglement," Phys. Rev. Lett. **106**, 053901 (2011).
81. M. Hall, J. Altepeter, and P. Kumar, "All-optical switching of photonic entanglement," New J. Phys. **13**, 105004 (2011).
82. T. M. Rambo, J. B. Altepeter, and P. Kumar, "Functional quantum computing: An optical approach," Phys. Rev. A **93**, 052321 (2016).
83. A. Barenco, C. H. Bennett, R. Cleve, D. P. DiVincenzo, N. Margolus, P. Shor, T. Sleator, J. A. Smolin, and H. Weinfurter, "Elementary gates for quantum computation," Phys. Rev. A **52**, 3457 (1995).
84. G. W. Lin, X. B. Zou, X. M. Lin, and G. C. Guo, "Robust and fast geometric quantum computation with multiqubit gates in cavity QED," Phys. Rev. A **79**, 064303 (2009).
85. C. P. Yang, S. B. Zheng, and F. Nori, "Multiqubit tunable phase gate of one qubit simultaneously controlling n qubits in a cavity," Phys. Rev. A **82**, 062326 (2010).
86. C. P. Yang, Q. P. Su, F. Y. Zhang, and S. B. Zheng, "Single-step implementation of a multiple-target-qubit controlled phase gate without need of classical pulses," Opt. Lett. **39**, 3312–3315 (2014).
87. C. H. Bai, D. Y. Wang, S. Hu, W. X. Cui, X. X. Jiang, and H. F. Wang, "Scheme for implementing multitarget qubit controlled-NOT gate of photons and controlled-phase gate of electron spins via quantum dot-microcavity coupled system," Quantum Inf. Process. **15**, 1485–1498 (2016).
88. M. Šašura and V. Bužek, "Multiparticle entanglement with quantum logic networks: Application to cold trapped ions," Phys. Rev. A **64**, 012305 (2001).
89. T. H. Taminiau, J. Cramer, T. van der Sar, V. V. Dobrovitski, and R. Hanson, "Universal control and error correction in multi-qubit spin registers in diamond," Nat. Nanotechnol. **9**, 171–176 (2014).
90. T. Beth and M. Rötteler, "Quantum algorithms: Applicable algebra and quantum physics," in *Quantum Information*, G. Alber, T. Beth, M. Horodecki, P. Horodecki, R. Horodecki, M. Rötteler, H. Weinfurter, R. Werner, and A. Zeilinger, eds (Springer, 2001), pp. 96–150 .
91. Y. Lu, G. R. Feng, Y. S. Li, and G. L. Long, "Experimental digital quantum simulation of temporal-spatial dynamics of interacting fermion system," Sci. Bull. **60**, 241–248 (2015).

1. Introduction

Quantum computation works as a pattern of parallel computing and it has a stronger capacity in information processing. It can speed up factorizing a large number [1] and searching data [2, 3]. The ultimate aim of quantum computation is the realization of quantum computer and the key element of a quantum computer is the quantum controlled-NOT (CNOT) gate (or its equivalency, the quantum controlled-phase gate). Many physical architectures have been proposed to implement quantum computation, such as photons [4–13], atoms [14–22], quantum dots [23–28], diamond nitrogen-vacancy defect centers [29, 30], nuclear magnetic resonance [31–37], and so on. Photon is an idea information carrier as it has a high transmission speed, a weak interaction with its environment, and a low cost for its preparation. Moreover, a photon system can have multiple degrees of freedom (DOF) which can be used in various quantum information processing tasks [38–42]. A state of a photon system being simultaneously entangled in several DOFs is referred to as a hyperentanglement, and its generation has been extensively researched both theoretically and experimentally [43–53]. The hyperentangled states of the photon systems can improve both the channel capacity and the security of quantum communication largely. The hyperparallel quantum computation is accomplished with the hyperentangled states of the photon

Optics EXPRESS

systems. The hyperparallel quantum computation can achieve the full potential of the parallel computing in quantum computation, and it can speed up quantum computing, save quantum resource, resist to noise, and will be useful for easy storage in the following process.

The first protocol for the hyperparallel quantum CNOT gate was proposed by Ren *et al*. [54] in 2013. In their protocol, a deterministic hyper-CNOT gate is constructed and it operates in both the spatial-mode and the polarization DOFs for a photon pair simultaneously. Up to now, several hyperparallel quantum gate protocols have been proposed, including the hyperparallel CNOT gate on a two-photon system with two DOFs and the hyperparallel Toffoli gate on a three-photon system with two DOFs [55–58]. A deterministic (hyperparallel) photonic quantum gate can be completed with nonlinearity interaction, which can be provided by a matter qubit such as an artificial atom trapped in a microcavity. The electron spin in a GaAs-based or InAs-based charged quantum dot (QD) trapped in a double-sided microcavity is an attractive matter qubit [26, 59]. Utilizing the technique of spin echo, the electron spin coherence time of a charged QD can be maintained for more than 3 μs [60, 61], and the electron spin relaxation time can be longer ($\sim ms$) [62, 63]. The techniques of fast preparing the superposition states of an electron spin in a singly charged QD [64, 65], fast manipulating the electron spin in a charged QD [66–69], and detecting the state of the electron spin in a charged QD [70] have been realized. Moreover, it is easy to embed a charged QD into a solid-state microcavity.

In the ideal case, the QD-microcavity system can provide a perfect nonlinear interaction which can be used to construct a unity-fidelity deterministic (hyperparallel) photonic quantum gate. When it turns into the realistic condition, the nonlinear interaction is not perfect, which will reduce the fidelity of the quantum gate. Fidelity, which is the description of the quality of the quantum gate, is defined as $F = |\langle\Psi_r|\Psi_i\rangle|^2$, where $|\Psi_r\rangle$ and $|\Psi_i\rangle$ are the realistic final state and the ideal final state, respectively. In the realistic condition, $|\Psi_r\rangle \neq |\Psi_i\rangle$, which means there would be some errors in the final result of a quantum gate and leads to a non-unity fidelity. For a quantum CNOT gate, there would be bit-flip errors in the realistic condition and the fidelity would be non-unity. Specifically speaking, for a quantum CNOT gate, $|\Psi_0\rangle = (a_1|0\rangle_c + a_2|1\rangle_c)(b_1|0\rangle_t + b_2|1\rangle_t)$ represents the initial state of the system, where the subscripts c and t respectively represent the control qubit and the target qubit, and the coefficients satisfy $|a_1|^2+|a_2|^2 = 1$ and $|b_1|^2+|b_2|^2 = 1$. $|\Psi_i\rangle = a_1|0\rangle_c(b_1|0\rangle_t + b_2|1\rangle_t) + a_2|1\rangle_c(b_2|0\rangle_t + b_1|1\rangle_t)$ is the ideal final state after a quantum CNOT gate, which means the state of the target qubit is flipped when the control qubit is in the state $|1\rangle_c$, while it would not be changed when the control qubit is in the state $|0\rangle_c$. However, in the realistic condition, after the evolution of the system, the final state might be $|\Psi_r\rangle = a_1'|0\rangle_c(b_1|0\rangle_t+b_2|1\rangle_t)+a_2'|1\rangle_c(b_2|0\rangle_t+b_1|1\rangle_t)+a_3'|0\rangle_c(b_2|0\rangle_t+b_1|1\rangle_t)+a_4'|1\rangle_c(b_1|0\rangle_t+b_2|1\rangle_t)$, which means there is a possibility that the state of the target qubit is not flipped when the control qubit is in the state $|1\rangle_c$ and the state of the target qubit is flipped when the control qubit is in the state $|0\rangle_c$. The coefficients a_1', a_2', a_3', and a_4' and the fidelity of the quantum CNOT gate are affected by the parameters of the photon and the QD-microcavity system. That is to say, in a quantum CNOT gate together with a hyperparallel quantum CNOT gate, bit-flip errors can happen in the realistic condition, which would be reflected by the non-unity fidelity. As the importance of improving the fidelity of a quantum gate, the research in quantum gates with a robust fidelity has attracted much attention and several interesting schemes of quantum gates for atom systems [19–21] and QD systems [28] with robust fidelities have been proposed.

In this paper, we give an original approach to construct the universal self-error-corrected hyperparallel photonic quantum CNOT gate working on a two-photon system in both the polarization and the spatial-mode DOFs. In this gate, the state of one photon in the polarization and the spatial-mode DOFs controls the state of the other photon in the polarization and the spatial-mode DOFs simultaneously, which is equal to two identical quantum CNOT gates operating simultaneously on the systems in one DOF. It can speed up quantum computing, reduce the quantum resource consumed largely, resist to noise, and simplify the storage of quantum

Optics EXPRESS

information in a practical application. More interestingly, it can prevent the bit-flip errors arising from the nearly realistic imperfect nonlinear interaction of the QD-microcavity system. Its self-error-corrected pattern prevents bit-flip errors from happening in the gate, guarantees its fidelity robust, and relaxes its requirement for the realistic parameters. This self-error-corrected hyperparallel photonic quantum CNOT gate also works in a failure-heralded way. Meanwhile, we generalize this approach of the self-error-corrected hyperparallel photonic quantum CNOT gate working on a two-photon system to achieve the self-error-corrected hyperparallel photonic quantum CNOT^N gate working on a multiple-photon system, which also works in a failure-heralded way. These good features make this scheme more useful in the hyperparallel photonic quantum computation and the multiple-photon hyperentangled-state generation for quantum communication in the future.

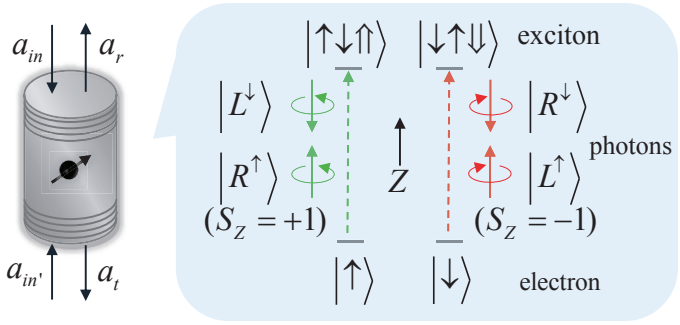

Fig. 1. Schematic diagrams for a singly charged QD in a double-sided microcavity, the relevant energy levels, and the optical transitions. Z represents the quantization axis (microcavity Z axis). $|R^{\uparrow}\rangle$ ($|R^{\downarrow}\rangle$) and $|L^{\uparrow}\rangle$ ($|L^{\downarrow}\rangle$) represent the right-circularly polarized photon and the left-circularly polarized photon propagating along (against) the normal direction of the microcavity Z axis, respectively.

2. Nonlinear interaction between a circularly polarized photon and a QD in a double-sided microcavity

A singly charged electron In(Ga)As QD or a GaAs interface QD is set at the wave loop of a double-sided microcavity. The reflection coefficients of the bottom and the top distributed Bragg reflectors of the double-sided microcavity are the same. An excess electron is injected into the QD. After the optical excitation by a circularly polarized photon, an exciton X^- consisting of two electrons bound to one heavy hole with negative charges is created. According to Pauli's exclusion principle, the circularly polarized photon $|L^{\downarrow}\rangle$ or $|R^{\uparrow}\rangle$ ($S_z = +1$) can only realize the transition from $|\uparrow\rangle$ to $|\uparrow\downarrow\Uparrow\rangle$, and the circularly polarized photon $|R^{\downarrow}\rangle$ or $|L^{\uparrow}\rangle$ ($S_z = -1$) can only realize the transition from $|\downarrow\rangle$ to $|\downarrow\uparrow\Downarrow\rangle$, as shown in Fig. 1.

The dipole interaction process can be represented by Heisenberg equations of motion for the annihilation operator $\hat{a}$ of the microcavity mode and the dipole operator $\hat{\sigma}_-$ of the exciton X^-. The Heisenberg equations in the interaction picture and the input-output relationships are

Optics EXPRESS

described as [71]

$$\begin{aligned}
\frac{d\hat{a}}{dt} &= -[i(\omega_c-\omega)+\kappa+\frac{\kappa_s}{2}]\hat{a}-g\hat{\sigma}_- -\sqrt{\kappa}(\hat{a}_{in'}+\hat{a}_{in})+\hat{H},\\
\frac{\hat{\sigma}_-}{dt} &= -[i(\omega_{X^-}-\omega)+\frac{\gamma}{2}]\hat{\sigma}_- -g\hat{\sigma}_z\hat{a}+\hat{G},\\
\hat{a}_r &= \hat{a}_{in}+\sqrt{\kappa}\hat{a},\\
\hat{a}_t &= \hat{a}_{in'}+\sqrt{\kappa}\hat{a}.
\end{aligned} \tag{1}$$

Here g is the coupling strength between the X^- and the microcavity. ω, ω_c, and ω_{X^-} are frequencies of the photon, the microcavity, and X^- transition, respectively. γ, κ, and κ_s represent X^- dipole decay rate, the microcavity decay rate, and the microcavity leaky rate, respectively. $\hat{H}$ and $\hat{G}$ are noise operators. $\hat{a}_{in}$, $\hat{a}_{in'}$, $\hat{a}_r$, and $\hat{a}_t$ are the input and output field operators. In the weak excitation approximation ($\langle\hat{\sigma}_z\rangle=-1$), after the nonlinear interaction between the circularly polarized photon and the QD-microcavity system, the reflection coefficient r and the transmission coefficient t can be described by [26, 72]

$$r = 1+t, \qquad t = -\frac{\kappa[i(\omega_{X^-}-\omega)+\frac{\gamma}{2}]}{[i(\omega_{X^-}-\omega)+\frac{\gamma}{2}][i(\omega_c-\omega)+\kappa+\frac{\kappa_s}{2}]+g^2}. \tag{2}$$

If the circularly polarized photon interacts with a cold microcavity, that is $g=0$, the reflection r_0 and the transmission t_0 coefficients can be written as

$$r_0 = 1+t_0, \qquad t_0 = -\frac{\kappa}{i(\omega_c-\omega)+\kappa+\frac{\kappa_s}{2}}. \tag{3}$$

The evolution rules for the nonlinear interaction between the circularly polarized photon and the QD in a double-sided microcavity in the realistic condition can be described as [26]

$$\begin{aligned}
|R^\uparrow\uparrow\rangle &\rightarrow r|L^\downarrow\uparrow\rangle+t|R^\uparrow\uparrow\rangle, & |L^\downarrow\uparrow\rangle &\rightarrow r|R^\uparrow\uparrow\rangle+t|L^\downarrow\uparrow\rangle,\\
|R^\downarrow\uparrow\rangle &\rightarrow t_0|R^\downarrow\uparrow\rangle+r_0|L^\uparrow\uparrow\rangle, & |L^\uparrow\uparrow\rangle &\rightarrow t_0|L^\uparrow\uparrow\rangle+r_0|R^\downarrow\uparrow\rangle,\\
|R^\downarrow\downarrow\rangle &\rightarrow r|L^\uparrow\downarrow\rangle+t|R^\downarrow\downarrow\rangle, & |L^\uparrow\downarrow\rangle &\rightarrow r|R^\downarrow\downarrow\rangle+t|L^\uparrow\downarrow\rangle,\\
|R^\uparrow\downarrow\rangle &\rightarrow t_0|R^\uparrow\downarrow\rangle+r_0|L^\downarrow\downarrow\rangle, & |L^\downarrow\downarrow\rangle &\rightarrow t_0|L^\downarrow\downarrow\rangle+r_0|R^\uparrow\downarrow\rangle.
\end{aligned} \tag{4}$$

3. Self-error-corrected hyperparallel photonic quantum CNOT gate

The hyperparallel photonic quantum CNOT gate working on a two-photon system in both the polarization and the spatial-mode DOFs, completes the task that when the polarization of photon a (the control qubit) is in the state $|L\rangle$, a bit flip takes place on the state in the polarization DOF of photon b (the target qubit), and simultaneously when the spatial mode of photon a is in the state $|a_2\rangle$, a bit flip takes place on the state in the spatial-mode DOF of photon b. The schematic diagram for our self-error-corrected hyperparallel photonic quantum CNOT gate is shown in Fig. 2. The QD-microcavity system is set in a basic block and the circularly polarized photon interacts with the QD-microcavity system through the basic block. In this way, the hyperparallel photonic quantum CNOT gate is constructed with a self-error-corrected pattern and works in a failure-heralded way.

The schematic diagram for the basic block is shown in the inset of Fig. 2. The electron spin in the QD in the microcavity is initially prepared in the state $|\varphi_+\rangle=\frac{1}{\sqrt{2}}(|\uparrow\rangle+|\downarrow\rangle)$ and a right-circularly polarized photon $|R\rangle$ is injected into the basic block from the input path. After the photon passing through BS and $H_{pi}(i=5,6)$, it interacts with the QD-microcavity system.

Optics EXPRESS

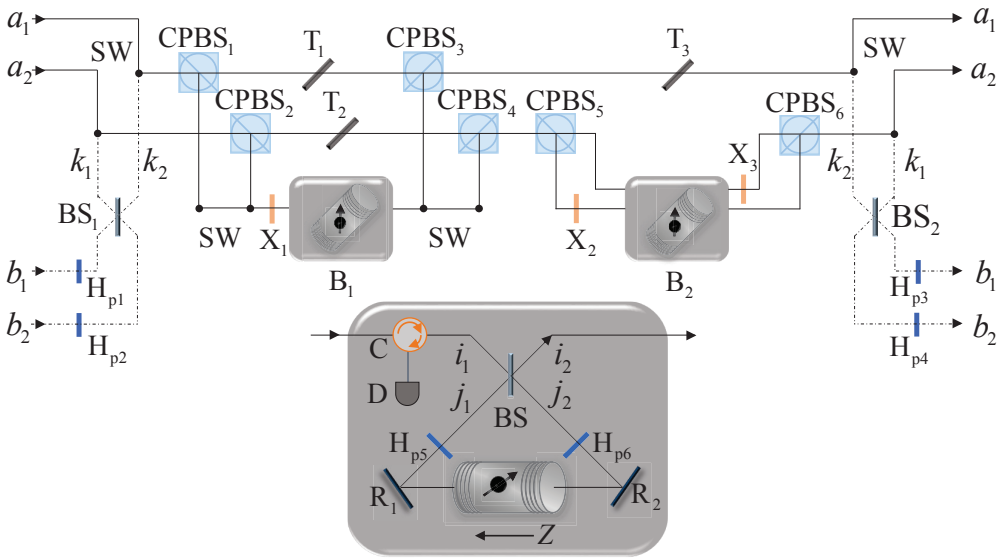

Fig. 2. Schematic diagram for hyperparallel photonic quantum CNOT gate with a self-error-corrected pattern. CPBS$_i$($i = 1 \sim 6$) is a circularly polarizing beam splitter which transmits the photon in the right-circular polarization $|R\rangle$ and reflects the photon in the left-circular polarization $|L\rangle$, respectively. BS$_i$($i = 1, 2$) is a 50 : 50 beam splitter which performs the spatial-mode Hadamard operation $[|b_1\rangle \rightarrow \frac{1}{\sqrt{2}}(|c_1\rangle + |c_2\rangle), |b_2\rangle \rightarrow \frac{1}{\sqrt{2}}(|c_1\rangle - |c_2\rangle)]$ on the photon. H$_{pi}$($i = 1 \sim 4$) is a half-wave plate which performs the polarization Hadamard operation $[|R\rangle \rightarrow \frac{1}{\sqrt{2}}(|R\rangle + |L\rangle), |L\rangle \rightarrow \frac{1}{\sqrt{2}}(|R\rangle - |L\rangle)]$ on the photon. X$_i$($i = 1 \sim 3$) is a half-wave plate which performs a bit-flip operation $[|R\rangle \rightarrow |L\rangle, |L\rangle \rightarrow |R\rangle]$ on the photon. T$_i$($i = 1 \sim 3$) is a partially transmitted mirror with the transmission coefficient T. SW is an optical switch which couples different photons into and out of the circuit of the photonic quantum gate sequentially and couples different spatial modes of a photon into and out of the basic block sequentially. B$_i$($i = 1, 2$) represents the basic block consisting of the QD$_i$($i = 1, 2$)-microcavity and the schematic diagram for the basic block is shown in the inset, in which C is an optical circulator which can route the photon into an appropriate path. BS is a 50 : 50 beam splitter. H$_{pi}$($i = 5, 6$) is a half-wave plate and completes the polarization Hadamard operation. R$_i$($i = 1, 2$) is a fully reflective mirror. D is a single-photon detector.

The rules of the nonlinear interaction between the photon and the QD-microcavity system in the realistic condition is governed by Eq. (4). And at last the photon passes through H$_{pi}$($i = 5, 6$) and BS again. The final state of the system consisting of the photon and the electron spin in the QD becomes

$$|\Phi\rangle_1 = D|R\rangle|i_1\rangle|\varphi_+\rangle + T|L\rangle|i_2\rangle|\varphi_-\rangle. \quad (5)$$

Similarly, when the electron spin in the QD in the microcavity is initially prepared in the state $|\varphi_-\rangle = \frac{1}{\sqrt{2}}(|\uparrow\rangle - |\downarrow\rangle)$, after a right-circularly polarized photon $|R\rangle$ passing through the basic block from the input path, the final state of the system becomes

$$|\Phi\rangle_2 = D|R\rangle|i_1\rangle|\varphi_-\rangle + T|L\rangle|i_2\rangle|\varphi_+\rangle. \quad (6)$$

$D = \frac{1}{2}(t + r + t_0 + r_0)$ and $T = \frac{1}{2}(t + r - t_0 - r_0)$ in Eqs. (5) and (6) are the reflection coefficient and the transmission coefficient for the basic block. Equations (5) and (6) describe the rules of

Optics EXPRESS

the interaction between the photon and the basic block. If the photon is reflected from the basic block with the probability of $|D|^2$, the polarization of the photon and the state of the electron spin in the QD would not be changed. The reflected photon would be detected by the single-photon detector and the following process would be terminated. If the photon is transmitted from the basic block with the probability of $|T|^2$, the polarization of the photon would be changed and the state of the electron spin in the QD would be changed as $[|\uparrow\rangle \rightarrow |\uparrow\rangle, |\downarrow\rangle \rightarrow -|\downarrow\rangle]$. The transmitted photon will be used in the following process, and the system consisting of the photon and the electron spin in the QD has an integrated coefficient T, which can guarantee the fidelity unity in the nearly realistic condition.

Based on the rules of the interaction between a right-circularly polarized photon $|R\rangle$ and a basic block, a self-error-corrected hyperparallel photonic quantum CNOT gate working in a failure-heralded way can be constructed. The detail principle can be described as follows in step by step.

Initially, the two electron spins in QD_1 and QD_2 are prepared in the states $|\varphi_+\rangle_1$ and $|\varphi_+\rangle_2$, and the two photons a and b are in the states $|\phi\rangle_a = (\alpha_1|R\rangle + \alpha_2|L\rangle)_a(\beta_1|a_1\rangle + \beta_2|a_2\rangle)$ and $|\phi\rangle_b = (\gamma_1|R\rangle + \gamma_2|L\rangle)_b(\delta_1|b_1\rangle + \delta_2|b_2\rangle)$, respectively. Here, $|\alpha_1|^2 + |\alpha_2|^2 = 1$, $|\beta_1|^2 + |\beta_2|^2 = 1$, $|\gamma_1|^2 + |\gamma_2|^2 = 1$, and $|\delta_1|^2 + |\delta_2|^2 = 1$.

First, photon a is injected into the circuit from the input path $a_i (i = 1, 2)$. After photon a passes through $CPBS_1$ and $CPBS_2$, in both of the two spatial modes $|a_1\rangle$ and $|a_2\rangle$, the wave packet in the left-circular polarization will pass through X_1 and the first basic block B_1, and the wave packet in the right-circular polarization will pass through T_1 and T_2. If there is a click of the single-photon detector in B_1, the process of the self-error-corrected hyperparallel photonic quantum CNOT gate fails and it is terminated. If the single-photon detector in B_1 does not click, the whole process will continue. The wave packet in the left-circular polarization and the wave packet in the right-circular polarization would reunion after passing through $CPBS_{3,4}$. In this time, the state of the hybrid system consisting of two photons a and b and two electron spins in QD_1 and QD_2 is changed from $|\Psi\rangle_0 = |\varphi_+\rangle_1|\varphi_+\rangle_2|\phi\rangle_a|\phi\rangle_b$ to $|\Psi\rangle_1$. Here

$$|\Psi\rangle_1 = T(\beta_1|a_1\rangle + \beta_2|a_2\rangle)(\alpha_1|R\rangle_a|\varphi_+\rangle_1 + \alpha_2|L\rangle_a|\varphi_-\rangle_1) \otimes |\phi\rangle_b|\varphi_+\rangle_2. \tag{7}$$

Subsequently, for the wave packet of photon a in the spatial mode $|a_1\rangle$, it transmits through T_3. For the wave packet of photon a in the spatial mode $|a_2\rangle$, after it passes through $CPBS_5$, the wave packet in the left-circular polarization transmits through X_2 and the second basic block B_2 in sequence, and the wave packet in the right-circular polarization transmits through the second basic block B_2 and X_3 in sequence. Similarly, if there is a click of the single-photon detector in B_2, the process of the self-error-corrected hyperparallel photonic quantum CNOT gate fails and it is terminated. If there is no click of the single-photon detector in B_2, the two wave packets of different polarizations in the spatial mode $|a_2\rangle$ reunion at $CPBS_6$, and the photon a comes out of the quantum circuit from path $a_i (i = 1, 2)$. And then Hadamard operations $[|\varphi_+\rangle \rightarrow |\uparrow\rangle, |\varphi_-\rangle \rightarrow |\downarrow\rangle]$ are respectively performed on the electron spins in QD_1 and QD_2. The state of the hybrid system is changed into

$$|\Psi\rangle_2 = T^2(\alpha_1|R\rangle_a|\uparrow\rangle_1 + \alpha_2|L\rangle_a|\downarrow\rangle_1)(\beta_1|a_1\rangle|\uparrow\rangle_2 + \beta_2|a_2\rangle|\downarrow\rangle_2) \otimes |\phi\rangle_b. \tag{8}$$

Second, photon b is injected into the circuit from the input path $b_i (i = 1, 2)$. After photon b passes through $H_{p1,2}$ and BS_1, the state of the hybrid system becomes

$$\begin{aligned} |\Psi\rangle_3 = {} & T^2(\alpha_1|R\rangle_a|\uparrow\rangle_1 + \alpha_2|L\rangle_a|\downarrow\rangle_1)(\beta_1|a_1\rangle|\uparrow\rangle_2 + \beta_2|a_2\rangle|\downarrow\rangle_2) \\ & \otimes [(\gamma_1'|R\rangle + \gamma_2'|L\rangle)_b(\delta_1'|b_1\rangle + \delta_2'|b_2\rangle)]. \end{aligned} \tag{9}$$

Here, $\gamma_1' = \frac{1}{\sqrt{2}}(\gamma_1 + \gamma_2), \gamma_2' = \frac{1}{\sqrt{2}}(\gamma_1 - \gamma_2), \delta_1' = \frac{1}{\sqrt{2}}(\delta_1 + \delta_2), \delta_2' = \frac{1}{\sqrt{2}}(\delta_1 - \delta_2)$. Subsequently, photon b passes through the circuit consisting of the optical elements and two basic blocks.

Optics EXPRESS

Similarly, if there is a click of the single-photon detector in B_1 or B_2, the process of the self-error-corrected hyperparallel photonic quantum CNOT gate fails and it is terminated. If there is no click, the whole process will continue. The polarization Hadamard and spatial-mode Hadamard operations are performed again on photon b by $H_{P3,4}$ and BS_2, respectively. Hadamard operations are performed on the two electron spins in QD_1 and QD_2 again. In this time, the state of the system consisting of two photons a and b and two electron spins in QD_1 and QD_2 is changed into

$$\begin{aligned}|\Psi\rangle_4 &= \frac{T^4}{2}[\alpha_1|R\rangle_a(\gamma_1|R\rangle+\gamma_2|L\rangle)_b+\alpha_2|L\rangle_a(\gamma_2|R\rangle+\gamma_1|L\rangle)_b]\\ &[\beta_1|a_1\rangle(\delta_1|b_1\rangle+\delta_2|b_2\rangle)+\beta_2|a_2\rangle(\delta_2|b_1\rangle+\delta_1|b_2\rangle)]|\uparrow\uparrow\rangle_{12}\\ &+\frac{T^4}{2}[\alpha_1|R\rangle_a(\gamma_1|R\rangle+\gamma_2|L\rangle)_b-\alpha_2|L\rangle_a(\gamma_2|R\rangle+\gamma_1|L\rangle)_b]\\ &[\beta_1|a_1\rangle(\delta_1|b_1\rangle+\delta_2|b_2\rangle)+\beta_2|a_2\rangle(\delta_2|b_1\rangle+\delta_1|b_2\rangle)]|\downarrow\uparrow\rangle_{12}\\ &+\frac{T^4}{2}[\alpha_1|R\rangle_a(\gamma_1|R\rangle+\gamma_2|L\rangle)_b+\alpha_2|L\rangle_a(\gamma_2|R\rangle+\gamma_1|L\rangle)_b]\\ &[\beta_1|a_1\rangle(\delta_1|b_1\rangle+\delta_2|b_2\rangle)-\beta_2|a_2\rangle(\delta_2|b_1\rangle+\delta_1|b_2\rangle)]|\uparrow\downarrow\rangle_{12}\\ &+\frac{T^4}{2}[\alpha_1|R\rangle_a(\gamma_1|R\rangle+\gamma_2|L\rangle)_b-\alpha_2|L\rangle_a(\gamma_2|R\rangle+\gamma_1|L\rangle)_b]\\ &[\beta_1|a_1\rangle(\delta_1|b_1\rangle+\delta_2|b_2\rangle)-\beta_2|a_2\rangle(\delta_2|b_1\rangle+\delta_1|b_2\rangle)]|\downarrow\downarrow\rangle_{12}.\end{aligned} \tag{10}$$

At last, the electron spins in QD_1 and QD_2 are measured in the orthogonal basis $[|\uparrow\rangle, |\downarrow\rangle]$. If the electron spin in QD_1 is in the state $|\downarrow\rangle_1$, an additional phase-flip operation $|L\rangle_a \rightarrow -|L\rangle_a$ is performed on photon a, and if the electron spin in QD_2 is in the state $|\downarrow\rangle_2$, an additional phase-flip operation $|a_2\rangle \rightarrow -|a_2\rangle$ is performed on photon a. Conditioned on the results of the measurement on the QD_1 and QD_2, the two-photon system, up to a single-photon rotation, is collapsed into the desired state with a success probability $T^8/4$ as follows

$$\begin{aligned}|\Psi\rangle_p &= [\alpha_1|R\rangle_a(\gamma_1|R\rangle+\gamma_2|L\rangle)_b+\alpha_2|L\rangle_a(\gamma_2|R\rangle+\gamma_1|L\rangle)_b]\\ &[\beta_1|a_1\rangle(\delta_1|b_1\rangle+\delta_2|b_2\rangle)+\beta_2|a_2\rangle(\delta_2|b_1\rangle+\delta_1|b_2\rangle)].\end{aligned} \tag{11}$$

From Eq. (11), one can see that there is a bit flip of the state on the polarization DOF for photon b when the polarization of photon a is in the state $|L\rangle_a$, and there is a bit flip of the state on the spatial-mode DOF for photon b when the spatial mode of photon a is in the state $|a_2\rangle$. Meanwhile, from Eq. (11), one can see that in the nearly realistic condition with imperfect nonlinear interaction, bit-flip errors do not happen in our hyperparallel photonic quantum CNOT gate, which means it works in the self-error-corrected pattern. Furthermore, from Eq. (10), one can see that $\frac{T^4}{2}$ is an integrated coefficient for the state of the two-photon system and the two electron spins in the QDs. Transmission coefficient T for the basic block is the function of transmission coefficient t (t_0) and reflection coefficient r (r_0) which are affected by the experimental parameters g, ω, ω_c, ω_{X^-}, γ, κ, and κ_s. That is to say, these experimental parameters would not affect the fidelity of the hyperparallel photonic quantum CNOT gate, which relaxes the requirement for experiment. Overall, the schematic diagram shown in Fig. 2 completes a self-error-corrected hyperparallel photonic quantum CNOT gate in the nearly realistic condition, which eliminates bit-flip errors, guarantees a robust fidelity, and relaxes the requirement for experiment, and its failure is heralded by the single-photon detectors.

4. Self-error-corrected hyperparallel photonic quantum CNOT^N gate

The previous approach completes the self-error-corrected hyperparallel quantum CNOT gate working on a two-photon system, which can be generalized to achieve the self-error-corrected

Optics EXPRESS

hyperparallel quantum CNOT^N gate working on a multiple-photon system. The self-error-corrected hyperparallel photonic quantum CNOT^N gate working on a multiple-photon system is completed with two basic blocks consisting of two QD-microcavity systems as auxiliaries, which is the same as the self-error-corrected hyperparallel quantum CNOT gate working on a two-photon system. Initially, the two electron spins in the two QDs are prepared in the states $|\varphi_+\rangle_1$ and $|\varphi_+\rangle_2$. The control photon a is in the state $|\phi\rangle_a = (\alpha_1|R\rangle + \alpha_2|L\rangle)_a(\beta_1|a_1\rangle + \beta_2|a\rangle)$ with $|\alpha_1|^2 + |\alpha_2|^2 = 1$ and $|\beta_1|^2 + |\beta_2|^2 = 1$. The N target photons $b^n(n = 1, 2, ..., N)$ are in the states $|\phi\rangle_{b^n} = (\gamma_1^n|R\rangle + \gamma_2^n|L\rangle)_{b^n}(\delta_1^n|b_1\rangle + \delta_2^n|b_2\rangle)_{b^n}$ with $|\gamma_1^n|^2 + |\gamma_2^n|^2 = 1$ and $|\delta_1^n|^2 + |\delta_2^n|^2 = 1$.

The schematic diagram shown in Fig. 2 can also be used to achieve the self-error-corrected hyperparallel photonic quantum CNOT^N gate. First, the control photon a is injected into the circuit from input path $a_i(i = 1, 2)$. During photon a passing through the circuit, if there is a click of the single-photon detector in the basic block B_1 or B_2, the process of self-error-corrected hyperparallel photonic quantum CNOT^N gate fails and it is terminated. If there is no click of the single-photon detector in B_1 nor B_2, with Hadamard operations respectively performed on the electron spins in QD_1 and QD_2, the state of the hybrid system is changed into

$$\begin{aligned}|\Psi^N\rangle_1 &= T^2(\alpha_1|R\rangle_a|\uparrow\rangle_1 + \alpha_2|L\rangle_a|\downarrow\rangle_1)(\beta_1|a_1\rangle|\uparrow\rangle_2 + \beta_2|a_2\rangle|\downarrow\rangle_2)\\ &\otimes|\phi\rangle_{b^1}|\phi\rangle_{b^2}\cdots|\phi\rangle_{b^N}.\end{aligned} \tag{12}$$

Second, the first target photon b^1 is injected into the circuit from the input path $b_i(i = 1, 2)$. Similarly, during photon b^1 passing through the circuit, if there is a click of the single-photon detector in the basic block B_1 or B_2 the process of self-error-corrected hyperparallel photonic quantum CNOT^N gate fails and it is terminated. If there is no click of the single-photon detector in B_1 nor B_2, the state of the hybrid system evolves into

$$\begin{aligned}|\Psi^N\rangle_2 &= T^4[\alpha_1|R\rangle_a|\uparrow\rangle_1(\gamma_1^1|R\rangle + \gamma_2^1|L\rangle)_{b^1} + \alpha_2|L\rangle_a|\downarrow\rangle_1(\gamma_2^1|R\rangle + \gamma_1^1|L\rangle)_{b^1}]\\ &[\beta_1|a_1\rangle|\uparrow\rangle_2(\delta_1^1|b_1\rangle + \delta_2^1|b_2\rangle)_{b^1} + \beta_2|a_2\rangle|\downarrow\rangle_2(\delta_2^1|b_1\rangle + \delta_1^1|b_2\rangle)_{b^1}]\\ &\otimes|\phi\rangle_{b^2}\cdots|\phi\rangle_{b^N}.\end{aligned} \tag{13}$$

Subsequently, the target photon from b^2 to b^N is injected into the circuit from the input path $b_i(i = 1, 2)$ one by one. The process is similar to the case that the click of the single-photon detector in B_1 or B_2 heralded the failure of the self-error-corrected hyperparallel photonic quantum CNOT^N gate. If there is no click of the single-photon detector in B_1 nor B_2, after the last target photon b^N exits from the output path $b_i(i = 1, 2)$, the state of the hybrid system is changed into

$$\begin{aligned}|\Psi^N\rangle_3 = T^{2(N+1)}&[\alpha_1|R\rangle_a|\uparrow\rangle_1(\gamma_1^1|R\rangle+\gamma_2^1|L\rangle)_{b^1}(\gamma_1^2|R\rangle+\gamma_2^2|L\rangle)_{b^2}\cdots(\gamma_1^N|R\rangle+\gamma_2^N|L\rangle)_{b^N}\\ &+\alpha_2|L\rangle_a|\downarrow\rangle_1(\gamma_2^1|R\rangle+\gamma_1^1|L\rangle)_{b^1}(\gamma_2^2|R\rangle+\gamma_1^2|L\rangle)_{b^2}\cdots(\gamma_2^N|R\rangle+\gamma_1^N|L\rangle)_{b^N}]\\ &[\beta_1|a_1\rangle|\uparrow\rangle_2(\delta_1^1|b_1\rangle+\delta_2^1|b_2\rangle)_{b^1}(\delta_1^2|b_1\rangle+\delta_2^2|b_2\rangle)_{b^2}\cdots(\delta_1^N|b_1\rangle+\delta_2^N|b_2\rangle)_{b^N}\\ &+\beta_2|a_2\rangle|\downarrow\rangle_2(\delta_2^1|b_1\rangle+\delta_1^1|b_2\rangle)_{b^1}(\delta_2^2|b_1\rangle+\delta_1^2|b_2\rangle)_{b^2}\cdots(\delta_2^N|b_1\rangle+\delta_1^N|b_2\rangle)_{b^N}].\end{aligned} \tag{14}$$

At last, Hadamard operations are performed on both the two electron spins in QD_1 and QD_2, and they are measured in the orthogonal basis $[|\uparrow\rangle, |\downarrow\rangle]$. If the electron spin in QD_1 and the electron spin in QD_2 are respectively in the state $|\uparrow\rangle_1$ and $|\uparrow\rangle_2$, the control photon a and the N target photons are in the state

$$\begin{aligned}|\Psi^N\rangle_p &= [\alpha_1|R\rangle_a(\gamma_1^1|R\rangle + \gamma_2^1|L\rangle)_{b^1}(\gamma_1^2|R\rangle + \gamma_2^2|L\rangle)_{b^2}\cdots(\gamma_1^N|R\rangle + \gamma_2^N|L\rangle)_{b^N}\\ &+\alpha_2|L\rangle_a(\gamma_2^1|R\rangle + \gamma_1^1|L\rangle)_{b^1}(\gamma_2^2|R\rangle + \gamma_1^2|L\rangle)_{b^2}\cdots(\gamma_2^N|R\rangle + \gamma_1^N|L\rangle)_{b^N}]\\ &[\beta_1|a_1\rangle(\delta_1^1|b_1\rangle + \delta_2^1|b_2\rangle)_{b^1}(\delta_1^2|b_1\rangle + \delta_2^2|b_2\rangle)_{b^2}\cdots(\delta_1^N|b_1\rangle + \delta_2^N|b_2\rangle)_{b^N}\\ &+\beta_2|a_2\rangle(\delta_2^1|b_1\rangle + \delta_1^1|b_2\rangle)_{b^1}(\delta_2^2|b_1\rangle + \delta_1^2|b_2\rangle)_{b^2}\cdots(\delta_2^N|b_1\rangle + \delta_1^N|b_2\rangle)_{b^N}].\end{aligned} \tag{15}$$

Optics EXPRESS

If the electron spins in QD_1 and QD_2 are respectively in the state $|\downarrow\rangle_1$ and $|\downarrow\rangle_2$, with respective additional phase-flip operations $|L\rangle_a \rightarrow -|L\rangle_a$ and $|a_2\rangle \rightarrow -|a_2\rangle$ on photon a, the photon system consisting of one control photon and N target photons is also projected into the state as shown in Eq. (15), which shows that there is a bit flip of the state on the polarization DOF for each target photon b^n when the polarization of the control photon a is in the state $|L\rangle_a$, and there is a bit flip of the state on the spatial-mode DOF for each target photon b^n when the spatial mode of the control photon a is in the state $|a_2\rangle$. Meanwhile, Eq. (15) is obtained under the consideration of nearly realistic condition, in which there are no terms show the happening of bit-flip errors. Furthermore, from Eq. (14), one can see $T^{2(N+1)}$ is an integrated coefficient for the state of the system, so the fidelity of hyperparallel photonic quantum CNOT^N gate is robust to the realistic experimental parameters, which relaxes the requirement for experiment. Overall, the approach of self-error-corrected hyperparallel quantum CNOT gate for a two-photon system is successively generalized to achieve the self-error-corrected hyperparallel quantum CNOT^N gate for a multiple-photon system, which eliminates bit-flip errors, guarantees a robust fidelity, and relaxes the requirement for experiment, and its failure is heralded by single-photon detectors.

5. Discussion and summary

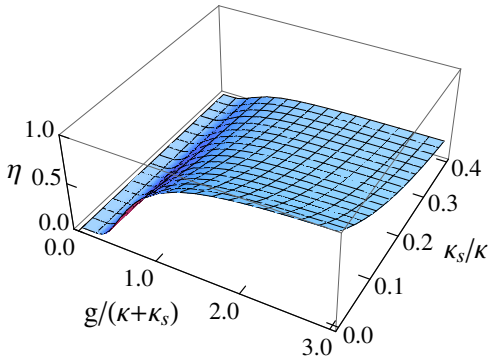

Fig. 3. The efficiency of our hyperparallel photonic quantum CNOT gate. $\omega = \omega_c = \omega_{X^-}$ and $\gamma/\kappa = 0.1$, which are experimentally achievable, are taken here.

The efficiency is defined as the ratio of the number of the output photons to the input photons. The efficiency of the self-error-corrected hyperparallel photonic quantum CNOT gate is described as

$$\eta = |T|^8, \tag{16}$$

which varies with the parameter $g/(\kappa + \kappa_s)$ and κ_s/κ as shown in Fig. 3. The non-unity efficiency of our proposal originates from photon loss. For example, there is a probability that a part of the photons are detected by single-photon detectors in the two basic blocks and these photons can also lose when passing through partially transmitted mirrors. For a practical scattering condition with $g/(\kappa + \kappa_s) = 3$ and $\kappa_s/\kappa = 0.1$, the efficiency of our self-error-corrected hyperparallel photonic quantum CNOT gate can reach 65.13%. With the same experimental parameters, the efficiencies of our self-error-corrected hyperparallel photonic quantum CNOT^2 gate and CNOT^3 gate can reach 52.56% and 42.42%, respectively.

The fidelities of our self-error-corrected hyperparallel photonic quantum CNOT gate and CNOT^N gate are robust to the experimental parameters g, ω, ω_c, ω_{X^-}, γ, κ, and κ_s, which relaxes the requirement for experiment. Exciton dephasing is a slight factor which would have a negative effect on the fidelity [73]. Taking the microcavity photon lifetime $\tau = 4.5ns$ and the electron

Optics EXPRESS

spin coherence time $\Gamma_2 \simeq 2.6\mu s$ [74] into account, the fidelity of every QD-microcavity system would be affected by an amount of $[1 - exp(-\tau/T_2)] \simeq 0.002$. Meanwhile, an imperfect mixing of heavy-light hole would lead to an imperfect optical selection which could affect the fidelity a little as well [75]. This imperfect mixing can be suppressed by engineering the shape and the size of QDs or by choosing the types of QDs.

The accomplishment of our self-error-corrected hyperparallel photonic quantum CNOT gate and CNOT^N gate requires the technique of the measurement on the state of the electron spin in the QD in the orthogonal basis $[|\uparrow\rangle, |\downarrow\rangle]$, which can be realized by measuring the helicity of the transmitted or reflected photon. Meanwhile, two transitions $|\uparrow\rangle \leftrightarrow |\uparrow\Uparrow\rangle$ and $|\downarrow\rangle \leftrightarrow |\downarrow\Downarrow\rangle$ couple to two microcavity modes with right- and left-circular polarization. So the microcavity for supporting two circularly polarized modes with the same frequency is required. This requirement can be satisfied [76–79]. For example, in 2012, Luxmoore *et al.* precisely tuned the energy split between the two circularly polarized microcavity modes to just 0.15 *nm* [76]. Also, the accomplishment of our scheme needs optical switches, which can couple different photons in and out the circuit of photonic quantum gate and couple different spatial modes of one photon in and out the circuit of the basic block. The performance of optical switch such as loss, delays, and the destruction on the photons, would affect the performance of our scheme. Fortunately, the suitable ultrafast optical switching device, that enables us to route single photons for quantum information processing, has been demonstrated. These switches exhibit a minimal loss, high speed performance, and a high contrast without disturbing the quantum state of photons that pass through them [80–82]. For instance, an ultrafast switch has been experimentally demonstrated and it completes the switch operation in $10ps$ [80], which is much shorter than the electron spin coherence time of a charged QD ($3\mu s$) [60, 61]. In our scheme, the failure-heralded character relies on the clicks of single-photon detectors in basic blocks. When there is a click of either single-photon detector, the process of self-error-corrected hyperparallel photonic CNOT gate and CNOT^N gate fails and it will be terminated. If the single-photon detector is perfect enough, no click of the single-photon detector marks the success of the scheme.

For establishing scalable quantum computation, multiqubit gates are useful. As well known, they can be constructed by two-qubit gates and single-qubit gates [83]. The direct realization of a multiqubit gate with one control qubit and multiple target qubits is essential and more efficient, and this topic has attracted much attention [18, 58, 84–87]. Fortunately, through directly generalizing our approach of self-error-corrected hyperparallel photonic quantum CNOT gate working on a two-photon system, the self-error-corrected hyperparallel photonic quantum CNOT^N gate working on a multiple-photon system is achieved, in which one photon in the polarization and the spatial-mode DOFs respectively controls all of the N target photons in the polarization and the spatial-mode DOFs. Our self-error-corrected hyperparallel photonic quantum CNOT^N gate is directly achieved rather than constructed by universal quantum gates, which has a potential in performing hyperentanglement preparation [88], error corrections [89], and quantum algorithms [90, 91].

In summary, we have presented the first scheme for designing the self-error-corrected hyperparallel photonic quantum CNOT gate, which relaxes the problem of the bit-flip errors happening in the quantum gate in the nearly realistic condition. The self-error-corrected pattern of our hyperparallel photonic quantum CNOT gate decreases the bit-flip errors, guarantees the robust fidelity, and relaxes the requirement of its experiment. Meanwhile, our self-error-corrected hyperparallel photonic quantum CNOT gate works in a failure-heralded way, as the clicks of single-photon detectors can mark the failure of the self-error-corrected hyperparallel photonic quantum CONT gate. Moreover, it can be generalized to the self-error-corrected hyperparallel photonic quantum CONT^N gate, which also works in the failure-heralded way. These features make our scheme more useful in quantum computation and the multi-photon hyperentangled-state generation in quantum communication in the future.

Optics EXPRESS

Funding

National Natural Science Foundation of China (NSFC) (11474026, 11674033, 11505007); Fundamental Research Funds for the Central Universities (2015KJJCA01).